AD-A130 696    CLOUD PHYSICS AND NUCLEATION THEORY: REVISIONS        1/1
               INDICATED BY NEW MEASUREME..(U) ARMY ARMAMENT RESEARCH
               AND DEVELOPMENT COMMAND ABERDEEN PROVI..  H R CARLON
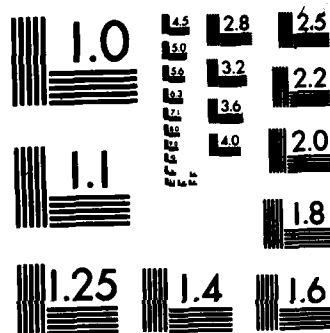UNCLASSIFIED   MAY 83 ARSSL-SP-81026                    F/G 4/2         NL

END

FILMED

DTIC

MICROCOPY RESOLUTION TEST CHART

NATIONAL BUREAU OF STANDARDS-1963-A

AD A130696

⑫

# CHEMICAL SYSTEMS LABORATORY

US Army Armament Research and Development Command
Aberdeen Proving Ground, Maryland 21010

SPECIAL PUBLICATION ARCSL-SP-81026

# CLOUD PHYSICS AND NUCLEATION THEORY: REVISIONS INDICATED BY NEW MEASUREMENTS OF THE ELECTRICAL CONDUCTIVITY OF EVAPORATION-HUMIDIFIED AIR

by

Hugh R. Carlon

Physics Branch
Research Division

May 1983

DTIC
ELECTE
JUL 2 1 1983
S
D
B

DTIC FILE COPY

83 07 20 091

SECURITY CLASSIFICATION OF THIS PAGE (When Data Entered)

| REPORT DOCUMENTATION PAGE | | READ INSTRUCTIONS BEFORE COMPLETING FORM |
|---|---|---|
| 1. REPORT NUMBER<br>ARCSL-SP-81026 | 2. GOVT ACCESSION NO. | 3. RECIPIENT'S CATALOG NUMBER |
| 4. TITLE (and Subtitle)<br>CLOUD PHYSICS AND NUCLEATION THEORY: REVISIONS INDICATED BY NEW MEASUREMENTS OF THE ELECTRICAL CONDUCTIVITY OF EVAPORATION-HUMIDIFIED AIR | | 5. TYPE OF REPORT & PERIOD COVERED<br>Special Publication<br>December 1980–December 1981 |
| | | 6. PERFORMING ORG. REPORT NUMBER |
| 7. AUTHOR(s)<br>Hugh R. Carlon | | 8. CONTRACT OR GRANT NUMBER(s) |
| 9. PERFORMING ORGANIZATION NAME AND ADDRESS<br>Commander, Chemical Systems Laboratory<br>ATTN: DRDAR-CLB-PO<br>Aberdeen Proving Ground, Maryland 21010 | | 10. PROGRAM ELEMENT, PROJECT, TASK AREA & WORK UNIT NUMBERS<br><br>Project 1L161101A91A |
| 11. CONTROLLING OFFICE NAME AND ADDRESS<br>Commander, Chemical Systems Laboratory<br>ATTN: DRDAR-CLJ-R<br>Aberdeen Proving Ground, Maryland 21010 | | 12. REPORT DATE<br>May 1983 |
| | | 13. NUMBER OF PAGES<br>39 |
| 14. MONITORING AGENCY NAME & ADDRESS(If different from Controlling Office) | | 15. SECURITY CLASS. (of this report)<br><br>UNCLASSIFIED |
| | | 15a. DECLASSIFICATION/DOWNGRADING SCHEDULE<br>NA |

16. DISTRIBUTION STATEMENT (of this Report)

Approved for public release; distribution unlimited..

17. DISTRIBUTION STATEMENT (of the abstract entered in Block 20, if different from Report)

18. SUPPLEMENTARY NOTES

19. KEY WORDS (Continue on reverse side if necessary and identify by block number)

20. ABSTRACT (Continue on reverse side if necessary and identify by block number)
A new theory of cloud physics is presented, based on new measurements of the electrical conductivity of moist air humidified by evaporation, combined with other measurements of related phenomena by mass spectrometry, infrared spectroscopy, and adiabatic expansion experiments in cloud chambers. It is shown that enormous populations of large, neutral molecular clusters of water molecules can exist in the vapor produced by evaporating liquid water, and at the vapor/liquid boundary layer that virtually all vapor initially can be clustered.

(Continued on reverse side)

DD FORM 1473 EDITION OF 1 NOV 65 IS OBSOLETE

## 20.    ABSTRACT (Contd)

cont

The neutral clusters dissociate into ions or serve as charge carriers to a small extent (given by the equilibrium dissociation constant or "ion product" of water) as measured by electrical conductivity using cells of a new design to monitor the temperature and humidity dependencies of the neutral cluster populations. The hydrogen bonds in the neutral clusters are strong absorbers of infrared radiation. Therefore, the activity of the neutral clusters in water vapor or moist air also can be monitored by infrared absorption and emission. The theory is supported by cluster modeling, as well as thermodynamic studies. It is shown that water droplet nucleation can be a temperature phenomenon and that supersaturations of more than perhaps one percent need not exist. The possible existence of a temperature-dependent energy barrier to nucleation in subsaturated conditions is demonstrated.

# PREFACE

The work described in this report was authorized under Project 1L161101A91A, In-House Laboratory Independent Research (ILIR), Chemical Munitions and Chemical Combat Support. This work was performed between December 1980 and December 1981.

Reproduction of this document in whole or in part is prohibited except with permission of the Commander, Chemical Systems Laboratory, ATTN: DRDAR-CLJ-R, Aberdeen Proving Ground, Maryland 21010. However, the Defense Technical Information Center and the National Technical Information Service are authorized to reproduce the document for United States Government. purposes.

The use of trade names in this report does not constitute an official endorsement or approval of the use of such commercial hardware or software. This report may not be cited for purposes of advertisement.

| Accession For | | |
|---|---|---|
| NTIS GRA&I | ☑ | |
| DTIC TAB | ☐ | |
| Unannounced | ☐ | |
| Justification | | |
| By | | |
| Distribution/ | | |
| Availability Codes | | |
| Dist | Avail and/or Special | |
| A | | |

Blank

4

# CONTENTS

Blank

6

# CLOUD PHYSICS AND NUCLEATION THEORY: REVISIONS INDICATED BY NEW MEASUREMENTS OF THE ELECTRICAL CONDUCTIVITY OF EVAPORATION-HUMIDIFIED AIR

## 1. INTRODUCTION

The theory of hydrogen bonding between water molecules was unknown to Aitken, Thomson, and other classical physicists when they formulated the basic theories from which modern cloud physics theory has evolved.[1] They *assumed* that liquid water evaporates into single molecules (monomers) as is the case with many unassociated liquids, that is, liquids that are not intermolecularly bonded. When C. T. R. Wilson published his landmark research on cloud chamber design and experimental results[2,3] in the late 1890's, this crucial bit of information – the hydrogen bonding of water still was missing. Thus Wilson, too, *assumed* that the explanation of his observations must lie in classical kinetic theory. Following this reasoning, the nucleation of cloud droplets in adiabatic expansion cloud chambers could only result from the collision and momentary association ("sticking") of individual monomers, with the "clusters" formed by this process repeatedly being impacted by other monomers in turn, until a tiny fraction of these clusters reached a "critical size" of perhaps 30 or more monomers. At this size, each cluster could then grow into a cloud droplet in the presence of sufficient water vapor.

Because of the nature of cluster growth by successive collisions of water monomers with clusters already momentarily formed in the vapor, kinetic theory predicts that each successive cluster size must of necessity represent a smaller fraction of the total vapor than does the next smaller cluster size from which it was formed by collision with a monomer. That is, the fraction of clusters of size "c" monomers could be represented by a Boltzmann-like distribution:

$$\frac{n_c}{n_1} = \exp - \frac{\Delta F}{k\theta} \qquad (1)$$

where $n_c/n_1$ is the fraction of c-sized clusters in the vapor (monomers, c = 1), k is Boltzmann's constant, $\theta$ is the absolute temperature, and $\Delta F$ is a nucleation energy term. This is a complex function of cluster size and other parameters, including the temperature and saturation ratio, "s" which is defined as %RH/100. This interpretation survives in modern homogeneous nucleation theory,[4] where $\Delta F$ is the familiar free energy of nucleation and varies with c in such a way that the dimer (c = 2) is the most populous cluster fraction $(n_2/n_1)$, followed by the trimer (c = 3, $n_3/n_1$) etc., until the least populous fraction, $n_*$, corresponds to a cluster size $c_*$ just large enough to permit droplet nucleation and growth.

But even Wilson[2,3] did not observe results compatible with kinetic theory as reflected in modern homogeneous nucleation theory.[2,3] Instead, he found huge populations of large, electrically neutral clusters and much smaller populations of singly charged clusters (which he later called "ions") always present in the saturated water vapor in his cloud chambers. By suddenly withdrawing the piston in a cloud chamber and causing adiabatic cooling to occur, Wilson saw droplets when the vapor was cooled to a final temperature where it could hold only one-fourth or one-fifth of the vapor that it could hold at the starting temperature. He observed two kinds of condensation; the first, which he called "rainlike," occurred at slightly smaller piston displacements, and the second, which he called

"cloudlike." The rainlike droplets, of which there were <100 per cm$^3$, were formed around ions as predicted by the Thomson equation.[1] The cloudlike droplets, which he knew to be electrically neutral, perplexed him because there were >10$^8$ of them per cm$^3$, they were much smaller than the rainlike droplets, and theory indicated that they had grown from cluster nuclei about three times larger in radius than the known molecular radius of water monomers. Knowing nothing about hydrogen bonding and constrained by the kinetic theory of gases, Wilson said:

> ". . . it is difficult to account for the immense number of these nuclei,
> otherwise than on the view that they actually are simply small aggregates
> of water molecules, such as may come into existence momentarily through
> encounters of the molecules. . . On this view the dimensions of the
> molecules cannot be small compared with 6 × 10$^{-8}$ centimeters. . ."

Wilson even suggested that the monomer radius might be in error by a factor of three! The concept that liquid water, which is almost completely hydrogen-bonded at normal atmospheric temperatures,[5] could produce vapor phase clusters at the evaporation boundary layer was completely foreign to Wilson. He therefore had to consider his observations as evidence of "supersaturation," even though in actual practice the rate at which droplets were produced in his cloud chambers could have been more a function of the rate at which he cooled the air by expansion, thereby producing condensed liquid water in his "nuclei" (clusters), than anything else. Also, for the near-ambient starting temperatures used by Wilson, four or five times the saturation vapor pressure (where s = 1.0) is required to provide enough water vapor to grow droplets large enough to be detected by optical means.[6] By Wilson's reckoning, this meant that "supersaturation" between s = 4 and s = 5 was required.

An elaborate formalism evolved from the classical physicists' assumption that only "supersaturation" of water vapor could account for observed water cloud nucleation phenomena. This formalism has evolved into cloud micro-physics and nucleation theory as it exists today. Still, cloud micro-physicists work with what is more of an art than a true science. Precise quantitative data are difficult to reproduce, and predictive modeling is unreliable. When hydrogen bonding of water was discovered[7] and the elaborate clustered structure of liquid water began to be appreciated, including beautiful geometric "clathrate" structures,[8] apparently no thought was given to the possible impact of these discoveries on existing kinetic models of liquid water evaporation and of water vapor produced by evaporation. It was recognized, however, that evaporating liquid water shows very poor agreement with kinetic models that work almost precisely for unassociated liquids.[9]

These discrepancies might have gone unrecognized indefinitely were it not for observations of a seemingly completely unrelated phenomenon anomalous infrared absorption by atmospheric water vapor. Gradually it was realized that the infrared "continuum" absorption observed between monomer lines in so-called atmospheric "window" wavelength regions could be due to hydrogen bonds in neutral water cluster distributions in moist air that absorb strongly as these wavelengths.[10-14] Infrared emission studies of wet cooling steam[15,16] in particular show excessive emission that can only be attributed to cluster activity. Clusters also seem to affect electromagnetic radiation at longer wavelengths extending to millimeter and microwavelengths, especially when clouds or fogs are present to ensure intimate vapor/liquid contact that enhances evaporation and recondensation.[17] Liquid water has an infrared opacity (absorption coefficient) that is 10$^3$ to 10$^4$ times greater than that of water vapor,[18] suggesting that the vapor could contain fractions of clusters of all sizes totaling 10$^{-4}$ to 10$^{-3}$ of the

monomer, or even more since the infrared continuum absorption is often 10 to 100 times larger than the absorption which can be attributed to the monomer between its strong absorption lines.[19] This seemed to indicate that, especially in hot damp air such as that containing saturated steam, nearly all of the vapor in contact with evaporating liquid water could be clustered. It was also found that the infrared continuum absorption of water vapor or moist air can be modeled almost precisely by an expression containing the dissociative equilibrium constant ("ion product") of water and the saturation vapor pressure at the temperature of interest.[11] But infrared calculations showed: (1) that the populations of neutral clusters needed to account for the infrared absorption were far larger than those predicted by homogeneous nucleation theory[4] but agreed with populations of these species reported by Wilson,[2,3] and (2) that the clusters must be large with typical mean sizes of $c = 20\text{-}30$ monomers, not dimers, trimers, etc. Again, this essentially agrees with Wilson's observations.

## 2. THEORY

2.1        Beginning with infrared data, the author has studied the problem clustering in water vapor over a period of about 15 years. However, a comprehensive theory to fit all observations could not have been developed without the aid of all of the experimental results described in this paper. Now the theory appears to be complete. The following discussion presents the essential elements of the new theory, followed by a presentation of experimental results to justify these elements.

2.1.1        Water vapor in contact with liquid water at equilibrium always contains huge populations of large neutral water clusters (sometimes called "embryos," as in homogeneous nucleation theory) that are produced by evaporation. These clusters are the "nuclei" that Wilson observed, that grow more than $10^8$ per $cm^3$ of optically detectable droplets when provided with enough vapor to condense on them by cooling to a lower "critical temperature."

2.1.2        These neutral clusters dissociate or otherwise acquire charge in a ratio on the order of $<100/>10^8$, according to the ion product of water, to form the ions that also were observed by Wilson and accounted for his rainlike condensation.

2.1.3        The amount of water vapor added ("supersaturation") is not really added at all, but is simply that excess amount of vapor which exists at the low temperature after cooling and is available to grow droplets to optically detectable size if the "critical supersaturation" point is reached or exceeded after sufficient sudden cooling of the vapor.

2.1.4        For the following reasons, there is no such thing as supersaturation of water vapor except at extremely low levels (fractions of one percent): saturation vapor pressure is a fundamental equilibrium property of water, and all excess vapor will almost immediately condense on nuclei in the air and on surfaces. Thus, by definition, the "critical (super)saturation" becomes $s = 1.0$, and "supersaturation" phenomena simply are temperature phenomena; i.e., the dropping of the temperature of moist air, thus forcing condensation.

2.1.5        The neutral clusters cannot be detected and measured directly except by condensation in a cloud chamber and growth to the cloudlike droplets such as was observed by Wilson, but their properties can be quantified by a number of modern techniques:

### a. Mass Spectrometry.[10]

It is assumed for purposes of discussion of the experimental results presented here that the ion source, e.g., a β-emitter, simply dissociates or charges existing clusters, rather than "building" clusters from monomers on ions. The latter technique is, of course, widely known and is extensively used to study the energetics of hydrated ions of all kinds; nothing contained in the present discussion has a negative impact on this technology in any way.

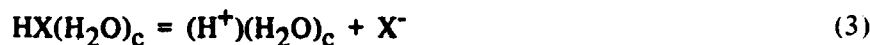### b. Infrared Absorption and Emission Spectroscopy.

This was the basis for first investigations of the new cloud physics theory. More about this will be said in the remaining discussion.

### c. Electrical Conductivity.

Measurements of moist air, if it is assumed that the neutral clusters in the vapor phase dissociate to a small extent (which can be greatly enhanced, e.g., by a β-radiation source) into ions, or become charge carriers, by reactions like:

$$(H_2O)_{c+d+1} = (H^+)(H_2O)_c + (OH^-)(H_2O)_d \tag{2}$$

or:

$$HX(H_2O)_c = (H^+)(H_2O)_c + X^- \tag{3}$$

where $X^-$ can be a negative ion or an electron, perhaps dislodged by the enhanced electron bombardment provided by a β-radiation source.

### d. Other Techniques.

These include studies of neutral cluster models and their expected frequencies and modes leading to electromagnetic radiation interactions,[13,14] and thermodynamic studies that can demonstrate agreement between cluster theory and observed thermodynamic properties of water.[13] Obviously, the latent heat of vaporization/condensation is especially important.

The elements of the new theory lead at once to some intriguing results. Because by definition here the "critical saturation" is s = 1.0 for condensation, the so-called "critical supersaturation" is given exactly by:

$$\ln (s)_{crit} = \left(\frac{373}{\theta}\right)^{5/2} - 1 \tag{4}$$

where 373 is the boiling point (°K) at 1 atmosphere. Thus when $\theta$ = 373 in equation 4, $\ln (s)_{crit}$ becomes zero in the Thomson equation:[1]

$$\frac{R\theta\sigma}{M} \ln (s)_{crit} = \frac{2T}{r} + \frac{dT}{dr} \tag{5}$$

where T is the surface tension, r is the cluster or droplet radius, $\sigma$ is the density of liquid water,

R is the gas constant, and M is the molecular weight. At the boiling point, the elusive term $dT/dr$ in equation 5, becomes simply:

$$\text{(at the boiling point) } \frac{dT}{dr} = -\frac{2T}{r} \tag{6}$$

and, presumably, $dT/dr$ can be found for other conditions as a function of $\Delta F$ (equation 1) and other classical parameters. Wilson and many other workers since Thomson have taken $dT/dr$ as zero, since they did not know how to characterize it. But this analysis suggests that $dT/dr$ is the key to the true behavior of water. An approximation widely used in cloud physics[1] is:

$$\ln (s)_{crit} = K\left(\frac{T}{\theta}\right)^{3/2} \cdot \frac{M}{\sigma} \tag{7}$$

"K" in equation 7 is troublesome because it is not constant, but keeps changing. However, in the new theory, equation 4 is exact.

Because of the author's assumption that $(s)_{crit}$ cannot exceed approximately 1.0, equation 4 is clearly misleading. If a temperature interpretation rather than a "supersaturation" interpretation is to be given to the nucleation of water droplets, then "critical" conditions should correspond to a temperature "barrier" condition which is the reciprocal of that shown in equation 4, namely,

$$\ln (s)_{barrier} = 1 - \left(\frac{373}{\theta}\right)^{5/2} \tag{8}$$

where equation 8 can be used with the standard tables of saturation vapor pressure for water to yield curves showing how the "barrier" might be interpreted. If further assumption is made that at the boiling point all vapor in the atmosphere in contact with liquid is completely clustered, then a new term for the fraction of the sum of all clusters of all sizes in water vapor, $(n_c)_v$, can be defined such that:

$$(n_c)_v = \frac{\sum_{2}^{*} (n_c)}{n_1} \quad \underset{\text{ing point}}{\overset{\text{at boil-}}{=}} \quad 1.0 \tag{9}$$

and

$$(n_c)_v = \frac{p_c}{p^0_v} = \frac{(s)(p^0_\theta)}{760} \tag{10}$$

where 760 torr is the saturation vapor pressure at the atmospheric boiling point, $p^0_\theta$ is the saturation vapor pressure at some temperature $\theta$ where "s" is specified, and $p_c$ (torr) is the partial pressure of all

vapor that is clustered under given equilibrium conditions. Defined in this way, $(n_c)_v$ thus is the pressure fraction of cluster in water vapor. Equations 8 through 10 allow figure 1 to be constructed. The fine, near-vertical dashed line to the right of figure 1 will be discussed later. The interpretation of figure 1 is as follows:

In figure 1, $(n_c)_v$ is plotted vs the saturation ratio, s, for several temperatures. The temperature curves (equation 10) have the slope $(s)^1$. From equation 8, the <u>barrier curve</u> is constructed. This is the heavy diagonal line on which the points representing temperatures used in its calculation are displayed. Thus, $(s)_{barrier}$ represents the <u>subsaturation</u> corresponding to a given temperature at 1 atm where "critical subsaturation" must occur. Now we must explain the physical significance of this curious concept.
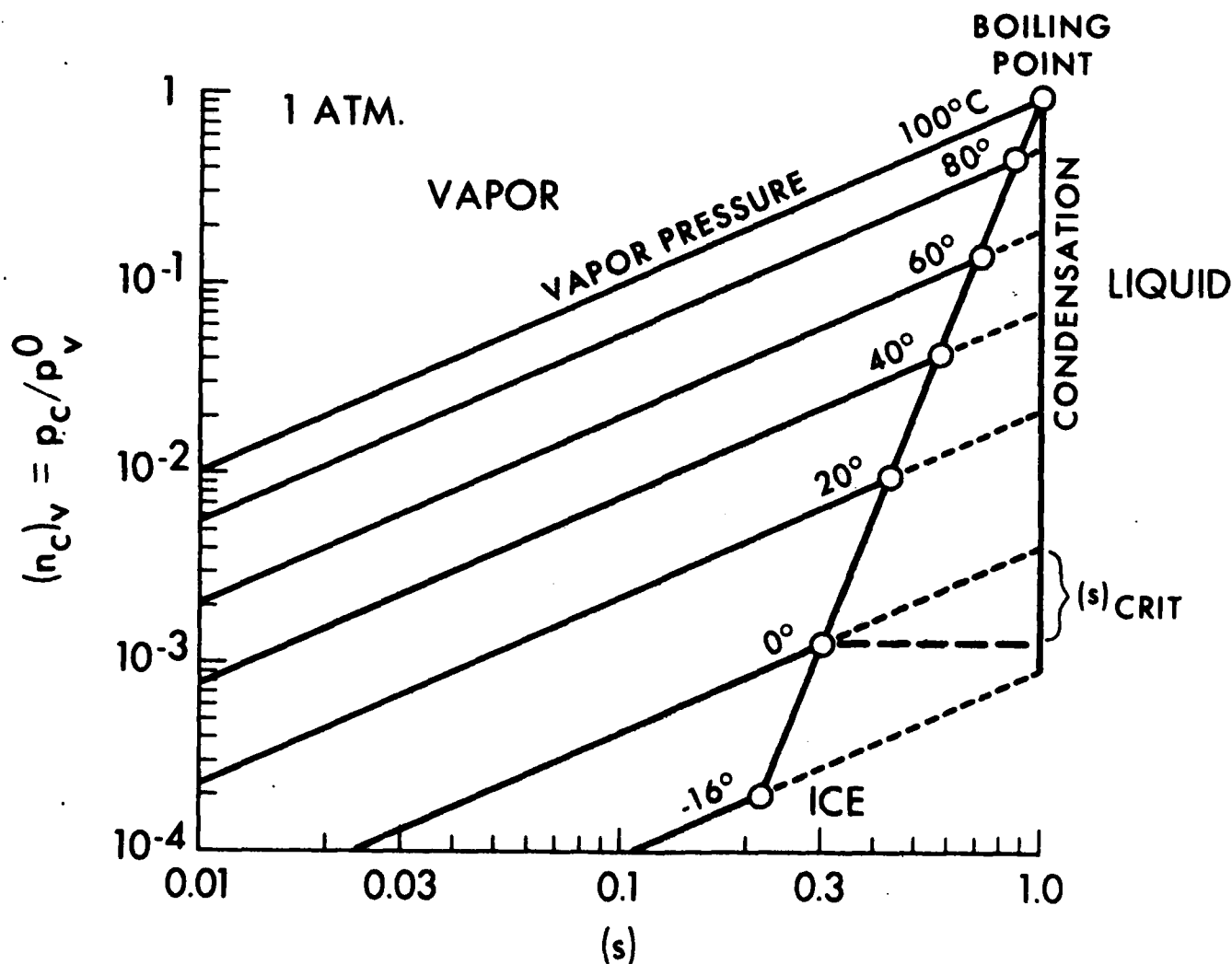


Figure 1. Fraction of Clustered Molecules in Water Vapor, $(n_c)_v$, vs Saturation Ratio (s = %RH/100) for Several Temperatures

This is the phase diagram of neutral water clusters in the vapor.

If the total number of clusters comprising the neutral cluster population per cc of vapor is designated $N_{cc}$, and the average size representative of all neutral clusters in the population is designated $c_u$, then the cluster fraction on the ordinate of figure 1 corresponding to a given constant-temperature curve will be:

$$(n_c)_v = \frac{(N_{cc}) (c_u)}{N_1} \tag{11}$$

where $N_1$ is the number of monomers per cc and is easily calculated from the gas laws. Figure 1 shows that as saturation ratio increases at constant temperature, $(n_c)_v$ also increases with a dependency $(s)^1$. Since $N_1$ also increases with an increase in $(s)^1$, this implies that the product $(N_{cc}) (c_u)$ actually has an $(s)^2$ dependency. Indeed, combining the gas law with equation 11 yields:

$$(n_c)_v = \frac{K (N_{cc}) (c_u) \, \theta \, M}{s \, p^o \, N_A} \tag{12}$$

where $N_A$ is Avogadro's number, and combining again with the right-hand part of equation 10 yields:

$$(N_{cc}) (c_u) = \frac{K (s \cdot p^o)^2 \, N_A}{\theta \, M} \tag{13}$$

Equation 13 is interesting for a number of reasons, but primarily because the infrared continuum absorption is attributed to the hydrogen bonds in vapor-phase neutral water clusters.[10] The number of infrared-absorbing hydrogen bonds per cc of vapor thus would be the product $(N_{cc})$ $c_u)$, times a factor which represents the ratio of hydrogen bonds to monomers in an "average" cluster, lying almost certainly in the numerical range ~1 to 3/2. It is well known that the infrared continuum absorption has a direct pressure-squared dependency and an inverse temperature dependency. This is precisely the behavior that would be expected from equation 13.

It is therefore clear that the product $(N_{cc})$ $(c_u)$ increases as $(s)^2$ increases in figure 1, as one moves to the right along a constant-temperature curve. Even before the barrier curve is reached at "$(s)_{barrier}$" (equation 8), we must try to sort out how $(N_{cc})$ and $(c_u)$ vary with respect to one another in order to give their product as shown in equations 11 through 13. One way to do this is to go directly to measurements by mass spectrometry of the neutral clusters present in the population under given conditions, assuming that the assumptions stated earlier are at least reasonably valid, i.e., that a $\beta$-radiation source, for example, will greatly enhance cluster dissociation into ions (equations 2 and 3), and that the ion mass spectra will give at least some idea of the nature of the neutral cluster size distribution in undisturbed moist air under given conditions. When mass spectra are taken for $H^+(H_2O)_c$ species at temperatures around 99°-100°C, like those in equations 2 and 3, near-Gaussian distributions of cluster sizes, c, are found which shift toward a smaller c with decreasing values of s, as shown in figure 2. The near-Gaussian distributions seem to justify the use of an average size, which now becomes a mean size, $c_u$, which is representative of the cluster size distribution in equations 11 to 13. At cluster sizes favoring clathrate formation,[8] larger populations smoothness of the distributions, unless one attempts to use saturated vapor samples warmer than 84°C, to be heated to 99°-100°C to obtain mass spectra. For example, in figure 2, the distribution is smooth for the 417 torr sample (= $p^o$ at 84°C) which when warmed to 100°C gives a saturation

13

ratio s = 1.0.[10] But when warmer saturated samples are heated to 100°C, it is found that the spectra begin to disintegrate at values of c ~47. This is consistent with the idea in figure 1, that the point at s = 1.0 and 100°C corresponds to the conditions necessary for the formation of a critically sized droplet, $c_*$ ~47, precisely as predicted by our formulas, under which the critical saturation is always s = 1.
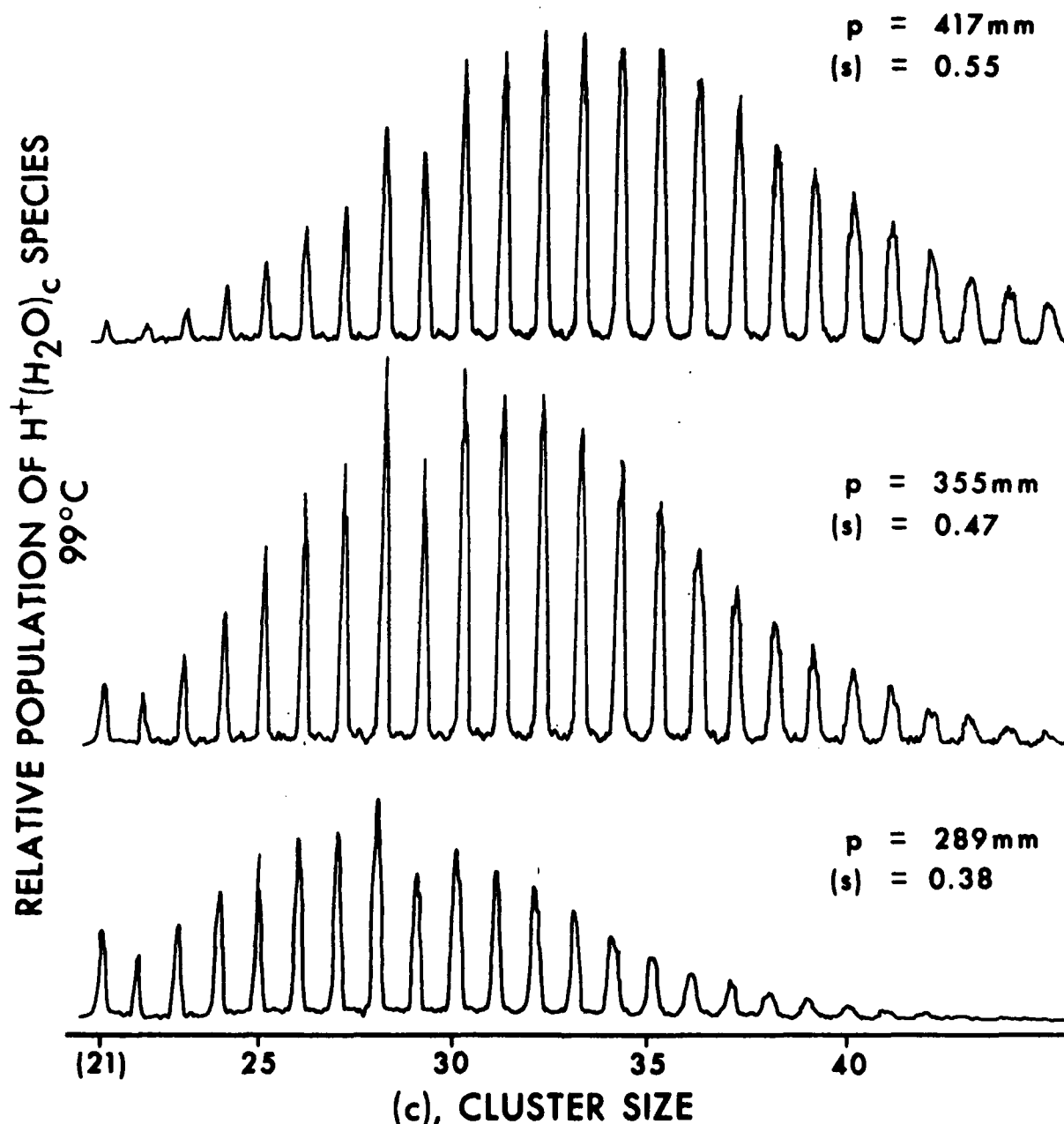


Figure 2. Mass Spectra of Ions $H^+(H_2O)_c$ in Moist Air
for Several Saturation Ratios at 99°C

When other mass spectra are taken, starting with a saturated moist air sample at room temperature and heating it at constant partial pressure to temperatures approaching 100°C, it is found that the peaks or mean sizes, $c_u$, of spectra like those in figure 2 shift through wide ranges of

$c_u$ as s becomes small. Some results obtained by heating saturated moist air from 28°C to 96°C are shown in figure 3.[10] Also shown in figure 3 are the constant temperature data from figure 2 and three other similar spectra (circular points), with the constant vapor pressure data (triangular points). A "knee" occurs in the solid curve of figure 3 at about $s$ = 0.2, which will be discussed later. A comparison of figure 3 with figure 1, for similar temperature and saturation ratios, thus allows some estimate to be made of the contribution of $c_u$ to the product $(N_{cc})$ $(c_u)$ and of values of $N_{cc}$ under these conditions, using equations 11 through 13. In general, it is found that values of $c_u$ can be represented by nearly vertical lines that can be drawn on figure 1, with values ranging from $c_u$ = ~10 above s = ~0.03, to $c_u$ = ~15 above s = ~0.15. But as the barrier curve is approached, the situation becomes confused and the $c_u$ values seem to "squeeze together" in ways still being investigated by the author until, by some mechanism, the critical cluster size for droplet growth is reached. At 100°C, $c_*$ ~47 for the condensation boundary, which of course is at s = 1 and is the right-hand solid line so labeled in figure 1.



KEY:

O CONSTANT TEMPERATURE, 99—100°C

△ CONSTANT VAPOR PRESSURE, HEATING FROM 28°C
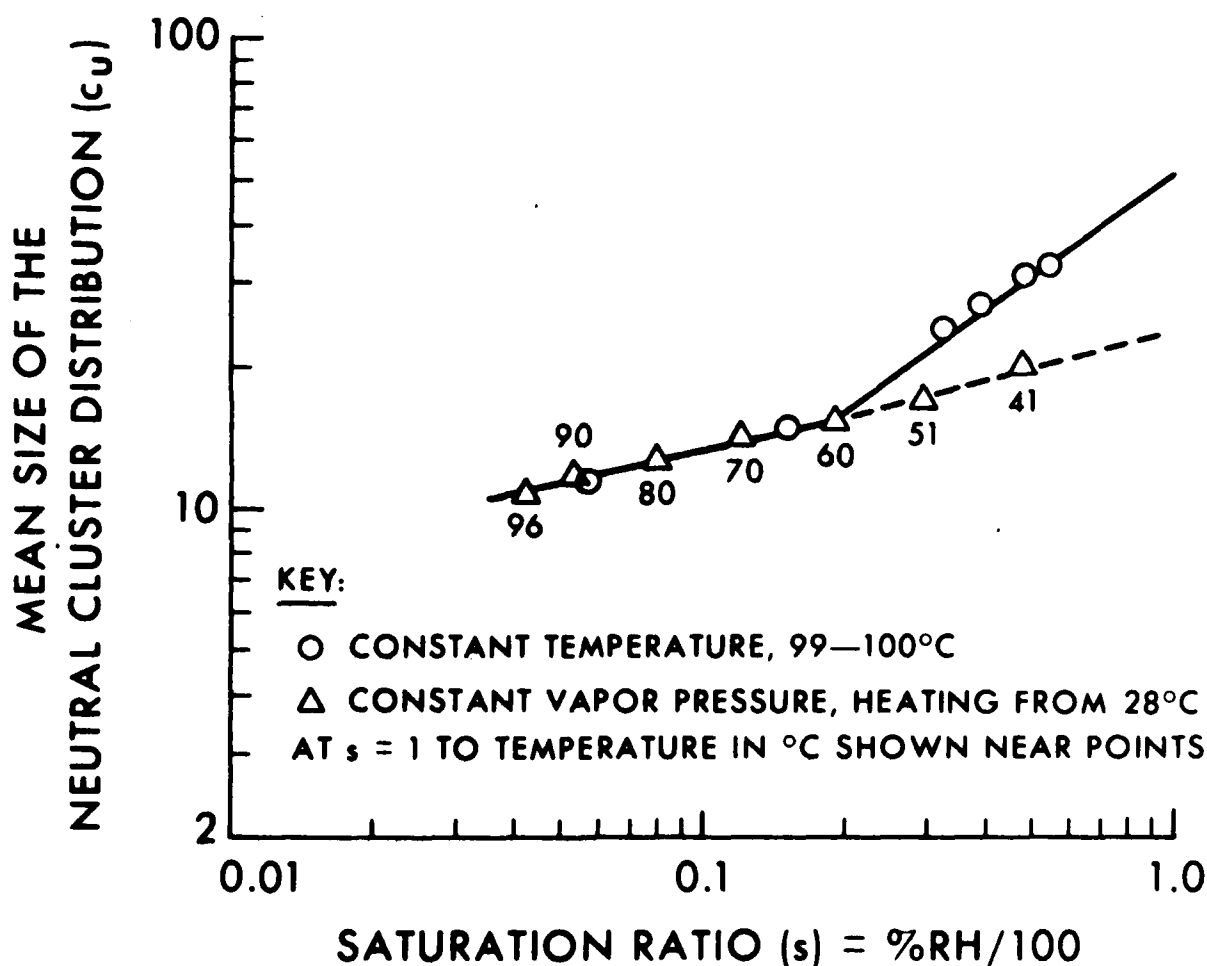
AT s = 1 TO TEMPERATURE IN °C SHOWN NEAR POINTS

Figure 3. Mean Size, $c_u$, of the Neutral Water Cluster
Distribution Inferred from Measured Ion Mass Spectra,
vs Saturation Ratio, for Constant Temperature of

Before proceeding with a further discussion of figure 1, we should discuss briefly the reasons why the ion mass spectra like those in figure 2 give such excellent agreement with the neutral cluster distributions that are known to be necessary to account for observed infrared continuum spectra and other phenomena. This agreement suggests that the neutral clusters merely serve as change carriers or lose only a small portion of their original mass (perhaps an $OH^-$ group or even an electron) during the supposedly rigorous process of being $\beta$-irradiated, forced through a tiny orifice into a high vacuum and instantaneously "frozen" to extremely low temperatures. Until recently the author was still attempting to resolve differences between classical kinetic theory and experimental observation,[10] arguing that if large neutral cluster distributions were present in moist air, they could not have gotten there by simple evaporation of the liquid, but by a more conventional route. This "accepted" route consisted of ions in the vapor causing monomers to be clustered to some mean size $c_u$, after which the charge was almost instantaneously lost, such that the resulting hydrogen-bonded neutral clusters, having much longer half-lives than the parent ions, were far more populous than the ions at any instant in time. Elaborate experiments were designed to test this hypothesis[20] that attempted to show that ion-induced neutral clusters could be generated in moist air using intense corona discharges, and thus enhanced the infrared continuum absorption as measured in a sensitive folded-path optical cell. These experiments produced no results and, like classical speed-of-light experiments, finally convinced the author to look at things from the other direction, that is, that the neutral clusters came from the evaporation of the liquid, not from the association of monomers. This also resolved the troublesome question of how such beautifully smooth and Gaussian mass spectra like those shown in figure 2 could be obtained by ion-induced clustering of monomers and charge neutralization. especially since the observed size distributions were peaked and had no Boltzmann-like skew whatsoever (equation 1).

Another interesting observation is that when equation 4 is solved for the lowest temperature for the equilibrium of vapor over liquid water ($257°K$), it produces a value of "$(s)_{crit}$" = 4.65, precisely in the range of values cited repeatedly by Wilson for condensation of droplets on neutral clusters or on their dissociative ions. Since this is the lowest vapor-phase temperature attainable for clusters evaporated from liquid water, it would seem to set a lower limit on "freezing" of these clusters even when subjected to extreme drops in temperature such as those found in expansion jets or expansion through orifices such as those used in mass spectrometers. The ion spectra (figure 2) might therefore be a far better representation of the sampled neutral cluster distributions than might otherwise be expected.[21,22] And indeed, infrared and other data do indicate that the cluster dependencies are almost precisely those seen in the ion spectra,[10] as has already been noted here.

Returning to figure 1, it is clear from this phase diagram that water vapor at some temperature (diagonal constant-temperature curves) that is gradually humidified will reach the barrier curve. For example, this occurs at $(s)_{crit}$ = ~0.3 at $0°C$, for which case $(n_c)_v$ = ~$10^{-3}$ (an excellent value of $(n_c)_v$, incidentally, to account for observed atmospheric infrared continuum absorption levels of water vapor near $0°C$ and at moderate humidities). If one moves along the $0°C$ line in figure 1 to the proposed barrier curve, one encounters a barrier to nucleation that otherwise would have occurred by following the extended (dashed) $0°C$ curve to the condensation line at $s = 1$. But the barrier has been encountered at a point that is still below the equilibrium value of $(n_c)_v$ at $0°C$ and $s = 1$ by the amount indicated by the bracket labeled "$(s)_{crit}$" to the right of the condensation line in figure 1. How is the saturation 1.0 (condensation) condition reached to produce droplet growth, from the point $s$ = ~0.3 and $\theta = 0°C$? There are two ways.

First, if the sample happens to be in an adiabatic expansion cloud chamber, the piston can be pulled out to provide the temperature drop necessary to overcome the nucleation barrier. The horizontal dashed line to the right of the 0°C point in figure 1 shows that at constant partial pressure this could be accomplished by expanding the sample enough to drop the temperature to about -13°C. The final conditions that must be met after expansion at constant partial pressure are easily deduced, using equation 8, from which:

$$(p^o)_{final} = (p^o)_\theta \exp\left[1 - \left(\frac{373}{\theta}\right)^{5/2}\right] \tag{14}$$

where $\theta$ is the barrier (starting) temperature from which nucleation will proceed to the final temperature. In the example given here, the barrier (starting) temperature is $\theta = 273°K$ where $p^o_{273}$ is 4.58 torr. The calculated saturation vapor pressure for the final temperature at s = 1.0 from equation 14 is $p^o_f = 1.404$ torr, which according to the tables of saturation vapor pressure corresponds to a final nucleation temperature of about -15°C. The slight temperature difference between -13°C for nucleation from figure 1, and -15°C from equation 14 can be accounted for by changes in the mean size of the cluster distribution ($c_u$) during cooling, since $c_u$ is sensitive both to temperature and to saturation ratio (see figure 3). Note that in the calculation of nucleation conditions from equation 14, only temperature and the tables of saturation vapor pressure are used. "Supersaturation" is not a factor in this proposed process and, indeed, it need not exist at all. These are temperature phenomena.

Clearly, from equation 14, at the boiling point $p^o_f = 760$, critical conditions are attained and free and continuous evaporation and recondensation occur between the vapor and the liquid at equilibrium. Saturations of 0.99999+ exist in the immediate boundary layer of the liquid.[9] The condition is thus achieved that all clusters in the liquid (which is nearly completely hydrogen-bonded)[5] interact with all clusters in the vapor, and the result is that all vapor is clustered at the boundary layer, justifying the location of the boiling point in figure 1, opposite $(n_c)_v = 1.0$.

The second way in which a constant-temperature vapor sample reaching the barrier curve in figure 1 can attain its equilibrium partial pressure and corresponding $(n_c)_v$ is fairly obvious. The product of neutral cluster population per $cm^3$ and mean cluster size must begin to increase at an accelerated rate with increasing "s." That is, the product $(N_{cc})(c_u)$ in equations 11 to 13 must increase by following the barrier curve abruptly upward to the final equilibrium partial pressure which corresponds to that value projected on the s = 1 condensation line, where it is intersected by the extension of the constant temperature curve (dashed in figure 1) for the constant temperature existing under the conditions of interest. The interpretation of this is that accelerated cluster growth begins at that temperature and value of "s" corresponding to the proposed nucleation barrier. Truly, this would be the beginning of "droplet" growth with the caveat that critical cluster size could be achieved for droplet nucleation unless (1) the condition s = 1 could be achieved by some route, and (2) enough excess vapor were available to grow droplets to a size large enough for optical detection.[6] The nucleation barrier in figure 1 mimics the dependencies upon s of the growth of water droplets at higher humidities. To be sure, the neutral clusters must compete for available water vapor with larger nuclei, including Aitken, continental, and maritime types which get a "head start" because the solution droplets they form have lowered saturation vapor pressures and thus can be nucleated when s <1. When an expansion cloud chamber is repeatedly recycled, the larger nuclei "rain out" and greater and greater piston displacements are necessary to reach temperatures low enough to overcome the nucleation barrier between the barrier curve and the vertical condensation line at s = 1 in figure 1. The last

17

nuclei to be activated and grown into droplets are the ions of the neutral clusters, which require a less extreme cooling because there is a subtractive ion charge term not shown in equation 5 for the Thomson equation for ions[1] and, finally, the huge populations of neutral clusters are themselves activated.

Even if clean water vapor is added during successive piston cycles of the cloud chamber so that s = 1 prior to the final step of activating neutral clusters, the physical limit discussed earlier still exists on the number of droplets that can be grown large enough for optical detection.[6] The maximum temperature range over which any cloud chamber can be operated is between 100°C and -16°C (figure 1). It follows from equations 8 and 14 and Carlon[6] that the number of droplets per cc that can be grown to radii barely large enough for optical detection, i.e., about 0.1 $\mu$m, has an upper limit of about $10^9$/cc, closely agreeing with the $>10^8$/cc figure reported by Wilson[2,3] that accounted for his cloudlike condensation on neutral nuclei (clusters).

It is also found, apparently fortuitously, that the temperature dedpendency of the nucleation barrier is given almost precisely by:

$$(n_c)_v \ _{barrier} = \exp 10.55 \left[ 1 - \left( \frac{373}{\theta} \right)^{3/2} \right] \tag{15}$$

The $\theta^{3/2}$ dependency of equation 7 is seen again, but in equation 15 it yields nearly exact values of the cluster fraction at all temperatures, suggesting that exp 10.55 might represent a combination of true constants of nature.

If one supplies heat or removes vapor, rather than adiabatically cooling a saturated vapor sample beginning on the barrier curve shown in figure 1, he will produce conditions represented by points to the left of the barrier curve. Saturated vapor at constant partial pressure, heated at 28°C from the barrier curve to higher temperatures, serves as an example. These were the conditions for which the triangular points were obtained in figure 3 corresponding to mean sizes of the cluster distributions at each temperature and saturation ratio. Since figures 1 and 3 have the same abscissa, the values of $c_u$ from figure 3 can be transferred to the appropriate locations on or between constant-temperature curves in figure 1. The locus of these points is found to be a near-horizontal line with a slight negative slope, for constant partial pressure, along which the mean cluster sizes are rather uniformly spaced as sequential integers. Some typical values were discussed earlier.

There is a wealth of infrared data supporting the analysis presented here, and much of it has already been referenced.[10-20] Bignell,[19] for example, found a "knee" and an upturn in data of the infrared continuum absorption vs the saturation that is extrapolable to the knee in cluster size shown in figure 3, where both of these effects presumably are connected with the barrier curve in figure 1. Bignell repeated his measurements and concluded that his data were correct. Many spectroscopists report a transition in atmospheric absorption for conditions corresponding to those near the barrier curve. The inference, of course, is that the fraction $(n_c)_v$ of clusters in water vapor produces absorption proportional to the numbers of hydrogen bonds in the clusters per cc, as was discussed in connection with the product $(N_{cc})$ $(c_u)$ in equations 11 and 12. It is also found that the dissociative equilibrium constant or "ion product" of water, $K_w$, can be used to describe the temperature dependence of the infrared continuum absorption[11] rather precisely, for reasons that will be discussed next.

From equations 2 and 3, if the populations $N_{cc}$ of neutral clusters are known (left sides of these equations) and if the extent of dissociation is known, it should be possible to deduce the populations of dissociative ions per cc, $I_{cc}$ (or at least of charge carriers per cc, if other mechanisms are involved). Since the equilibrium ion product of liquid water can be measured quite precisely as a function of temperature, and since the vapor and liquid clusters become identical at $(n_c)_v = 1.0$, when s = 1 at 100°C, the ion product could also describe the dissociation (or other charge-carrying mechanisms) of vapor-phase neutral clusters. For example, the equilibrium ion porduct of equation 3 is:

$$K_w = {}^a H^+(H_2O)_c \cdot {}^a X^- \qquad (16)$$

where "a" is the molar concentration of either species. Thys, the ion product for each ion pair can be given by $2\sqrt{K_w}$. The dissociative water ion cluster population per cc, $I_{cc}$, becomes:

$$I_{cc} = 2 k \sqrt{K_w} (N_{cc}) \qquad (17)$$

where k is a coefficient whose value depends on parameters including $c_u$ and $\theta$. $c_u$ also affects ion mobility, and thus this development suggests a technique to measure cluster size and mobility. The strong temperature dependence of $K_w$ can be calculated approximately from a rewritten form of an equation deduced by Holzapfel:[23]

$$K_w = \exp ( - 8.17 - 7156/\theta ) \qquad (18)$$

The author has carried out very careful measurements of actual $I_{cc}$'s in moist air over a range of values of s, including s = 1, using giant electrical conductivity cells of a new design that were fabricated specifically for this work.[24,25] The cells are compensated for insulator leakage so that measurements can be carried out to complete saturation. In fact, even in completely saturated moist air, the ion populations in the air between the cell plates are much larger than the populations on the insulators. The cells and measurements using them will be described in the next section. Chalmers[26] gives mobilities of u = 1 - 2 cm²/V-sec for water ion clusters of assumed sizes c = 10 to 12, which are much smaller than the ion clusters measured in our work by mass spectrometry (figure 2), especially for conditions near the barrier curve of figure 1. An average value of u = 0.6 cm²/V-sec is found to give consistent results in the following discussion.

If one wishes to use figure 1 directly to study measured values of $I_{cc}$ for agreement with the proposed theory, he must first correct the barrier curve for the strong temperature dependence of $\sqrt{K_w}$ as given in equations 17 and 18. This correction results in the nearly vertical, fine dashed curve in figure 1 just to the left of the vertical condensation line at s = 1. This fine dashed curve can be thought of as the barrier curve for $I_{cc}$ measurements vs s, although this is not strictly the case.

3.    EXPERIMENTAL PROCEDURE AND RESULTS

In an earlier paper,[24] the author reported that untreated room air humidified by boiling water could contain $10^6$ to $10^7$/cc of singly charged, hydrated ions like $H^+(H_2O)_c$, for which size distributions are shown in figure 2 for some typical conditions. Mobilities of about 0.6 cm²/V-sec are

19

appropriate for these, although Chalmers' value of 2 $cm^2$/V-sec was used in the earlier work.[26] It was also shown that these large ion populations could be maintained for an hour or more in closed containers after water vapor generation by boiling water had ceased. The ions in moist air were measured by two cells, one a large analytical cell, the other a much smaller cell having an insulator configuration identical to the large cell so that insulator effects could be studied independently as functions of humidity and temperature and could be used to correct the data so that values of $I_{cc}$ for the moist air only could be deduced. The large cell consisted of 40 parallel steel plates 41 cm on an edge spaced L = 0.66 cm apart on rod insulators. The effective plate area was determined as A = 6.6 × $10^4$ $cm^2$ by measuring the electrical capacitance of the cell with an electronic impendance bridge. The smaller cell had a much smaller effective area (A = 2600 $cm^2$), but the same plate spacing (L = 0.66 cm), and is shown in figure 4. Together, the cells allowed very sensitive measurements to be made of the electrical conductivity and, hence, of the ion populations $I_{cc}$ of moist air between the cell plates over a wide range of temperatures and humidities, including humidities approaching saturation (s = 1).

The original cells used insulators consisting of 8-mm-diameter resin-impregnated fiberglass rods with nylon spacers (nuts) 0.66 cm thick, as shown in figure 4. These materials were selected for their high electrical resistance, but were not the only materials tried over the 2-year period during which experimental cells were built and tested. Teflon insulators were also tried but seemed to give extremely troublesome surface effects and were abandoned in favor of the fiberglass rods which gave reproducible results and shunting resistances (leakages), that were negligible compared to those of typical moist air samples near ambient temperatures. The author's continuing work with both the fiberglass- and Teflon-insulated cells finally led him to the realization that the latter were not giving troublesome effects after all. In fact, they were simply giving accurate indications of phenomena that were not understood prior to the present work, and the fiberglass-insulated cells did not show these effects because they were leakier than the Teflon cells. The leakiness masked the phenomena reported in the present paper, especially at humidities approaching 100% (i.e., s = 1). Therefore, for the work reported here, the author used the original smaller cell refitted with Teflon insulator rods and the original nylon spacers as shown in figure 4, paired with a new analytical cell of an idential Teflon insulator configuration using the same nylon spacers. In the course of this work, it was found that the new cell could be made smaller (20 cm on an edge) and thus lighter and more compact, while still retaining excellent sensitivity. For this reason, the new Teflon-insulated cell, which also consisted of 40 plates, had an effective area determined by the impedance bridge of A = 1.4 × $10^4$ $cm^2$ while retaining the plate spacing of L = 0.66 cm.

Recent results with the Teflon-insulator cell pair have shown that the electrical conductivity of moist air is extremely dependent on its saturation ratio (s = %RH/100). These results also indicate that boiling is not necessary to generate large ion populations, but that simple evaporation will suffice. Studies of moist air and insulator conductivities simultaneously have shown unequivocally that the electrical conductivity of moist air is a much more important factor than has been previously recognized in space charge dissipation, especially in closed spaces. Accepted electrostatic theory[27] attributes certain phenomena to insulator leakage, such as the well-known humidity dependence of annoying static-electric shocks received by people moving and touching objects in dry heated rooms in wintertime. The electrical conductivity of moist air almost certainly explains these phenomena. Of course, earlier workers in the field had no reason to suspect the existence of huge populations of neutral water clusters in moist air, whose dissociative ions (equations 2 and 3) always exist when water vapor is in equilibrium with liquid water (which act directly as charge carriers). The experimental
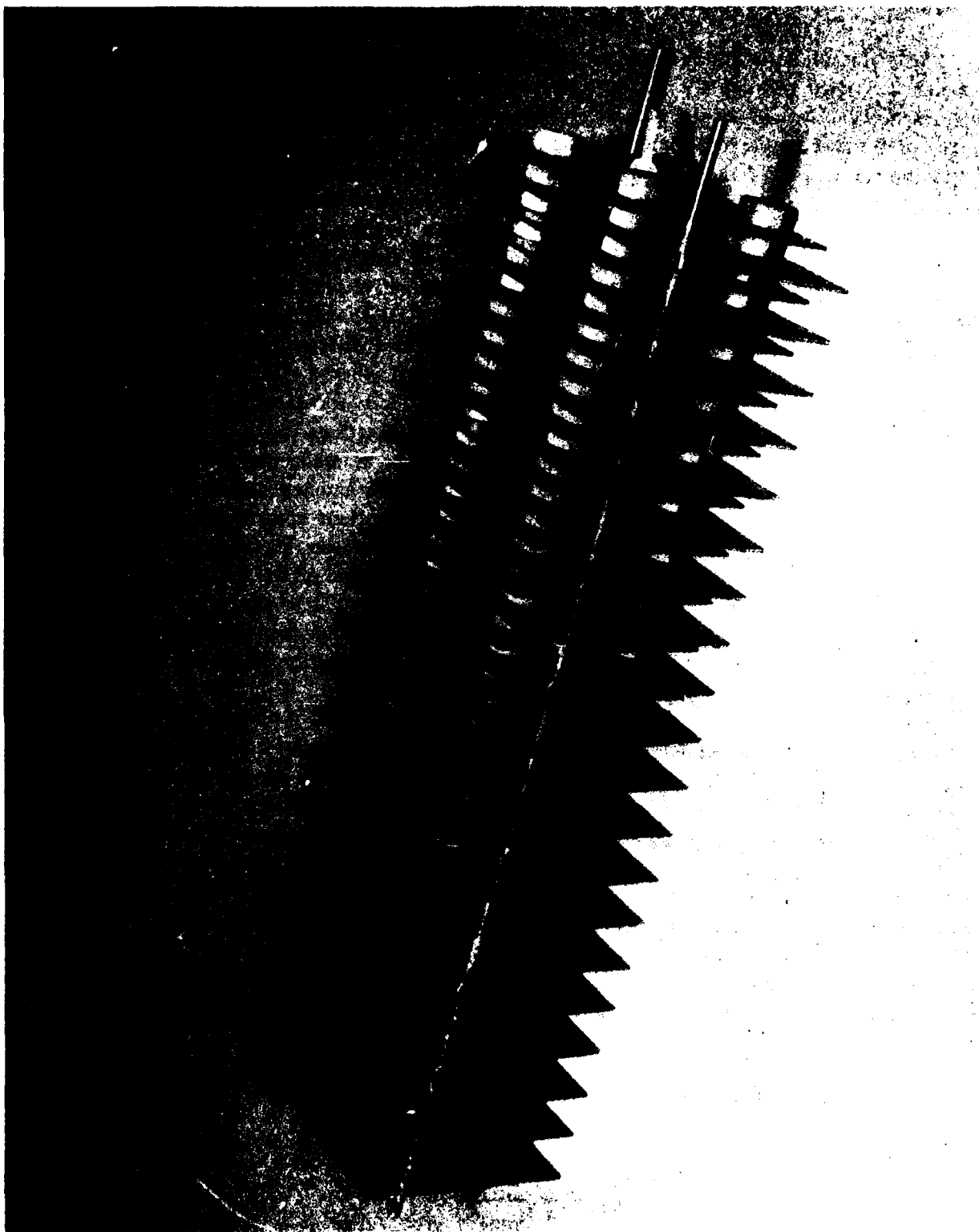
Figure 4. Close-up View of the Smaller Electrical
Conductivity Cell, Showing Construction Details

For scale, overall length is 29 cm.

evidence presented in earlier sections of this paper presents a strong case for this theory indeed, which will be strengthened by the additional results reported here.

The plates of both Teflon-insulated cells are supported by four Teflon rods, 8 mm in diameter, which are fitted through the plates near their corners and carry the nylon nuts used as spacers. A fifth set of spacers is carried on a length of Teflon tubing run through the centers of the plates for the length of the cell to prevent plate warping. Alternating plates are connected to either of two bus wires running the length of the cell (29 cm), somewhat in the fashion of an automotive storage battery but, in this case, with moist air as the electrolyte. When air is dry, its ion content at room temperature is typically $<10^3/cm^3$, and the electrical resistance (reciprocal conductance) of either cell is $>10^{11}$ $\Omega$. The sensitivity of the cells to ions in moist air between the plates is determined by the "cell factor," or ratio of plate spacing (L = 0.66 cm) to effective plate area, A, in $cm^2$. Thus, the cell factor of the large Teflon-insulated cell is L/A = 4.7 X $10^{-5}$ $cm^{-1}$, while the cell factor of the smaller cell is L/A = 2.5 X $10^{-4}$ $cm^{-1}$. This gives the two cells two different ranges of sensitivity, which will be shown to be very useful at higher temperatures and when s = 1, where ion populations $I_{cc}$ become enormous and the larger cell becomes saturated; i.e., it is too sensitive. Since both cell factors are known and the differences in their conductivity data functions can be solved simultaneously to determine the insulator leakage function, cell measurements can be made under conditions of complete saturation at temperatures of at least 50°C with high precision and repeatability. Repeated experimental trials have shown that insulator leakage is not an important contributor to the overall cell conductance, simply because under conditions such that the insulators become damp, the air between the plates still contains a much higher ion population than is found on the insulators. Intuitively, this makes perfect sense, since the insulator areas are miniscule compared to the cell plate areas exposed to the ions in the moist air between the plates. Therefore, the closer one comes to the boiling point at s = 1 by raising the temperature; the closer one will come to an identity of cluster structure and ion product between the vapor and liquid phases of water!

Either of the Teflon-insulated cells can, in fact, be used without compensation for insulator leakage under virtually all conditions. As will become apparent in the subsequent discussion, when measurements of $I_{cc}$ are made at temperatures above 50°C at s = 1, even the small cell becomes too sensitive and still smaller plate areas are needed to make such measurements. The author is presently fabricating a cell of the simplest possible configuration for sensitive measurements under such extreme conditions. This cell will consist of only two plates, 15 cm on an edge and slip-fitted onto a single 8-mm-diameter Teflon insulator rod through a hole near the center of one edge of each plate. In this way the plate spacing, L, can be adjusted at will, and insulator leakage will be kept to an absolute (and negligible) minimum. Thus the cell, or a set of similar cells set with different spacing, can be hung in the closed container used for $I_{cc}$ measurements and measurements can be made up to the boiling point.

The relationship between the ion population per cc of moist air, $I_{cc}$, and other parameters is given by:[24]

$$I_{cc} = \frac{L}{A} \frac{10^{-6}}{R_{meg}eu}$$  (19)

where L/A is the cell factor, $R_{meg}$ is the measured cell DC resistance in megohms, e is the value of electronic charge (1.6 X $10^{-19}$ C), and u is the mobility of a typical ion of size $c_u$, taken for much of this

work to be 0.6 cm$^2$/V-sec. Equation 19 and values of L/A for the cells given earlier show that the individual cell equations are:

$$\text{Large cell: } I_{cc} = -\frac{4.9 \times 10^8}{R_{meg}} \tag{20}$$

$$\text{Small cell: } I_{cc} = \frac{2.6 \times 10^9}{R_{meg}} \tag{21}$$

Because of the sensitivity of the cells, resistance can be measured by the unsophisticated method shown schematically in figure 5. An 11-megohm input impedance vacuum-tube voltmeter (VTVM) was placed in series with the cell under test and a regulated 0 to 400 vdc power supply so that the source voltage $E_b$ was divided between "E" across the 11 megohm VTVM load, and $E_c$ across the cell under test. The value of $1/R_{meg}$ for direct substitution in equations 20 and 21 is then given by:

$$\frac{1}{R_{meg}} = \frac{E}{11 \, (E_b - E)} \tag{22}$$

and it is even possible for a given source voltage setting $E_b$ to calibrate the voltmeter directly in $I_{cc}$ for a given cell, if such a calibration should be desired. For most measurements reported here,



Figure 5. Schematic Drawing Showing Method of Measuring
Cell Resistance with Vacuum-Tube Voltmeter

$E_b$ = 400 volts direct current, previously shown to have no effect on ion concentration.[24] The cells were placed in the 83 X 62 X 65 cm test cabinet shown in figure 6, where the cell shown was the large unit with fiberglass insulator with plates 41 cm on an edge (described earlier). The test cabinet had Lucite walls 0.95 cm thick but the space within the cabinet was unaffected in any detectable way by electrostatic charges on the walls which were, in any case, damp for most measurements and thus unable to maintain surface charge distributions. The smaller cabinet, 30 X 32 X 32 cm, shown in figure 6. was used in earlier work[24] for the generation of water vapor (steam) by boiling, but was

Figure 6. Test Cabinet and Instrumentation
For scale, large cell plates are 41 cm on an edge.

kept closed off for the experimental trials reported here. The access ports in the front of the cabinet were kept closed off during this work, and a muffin fan 10 cm in diameter inside the cabinet provided internal air circulation when needed at a face velocity of 4 m/sec, but an average recirculation velocity of moist air within the cabinet of 0.6 m/sec. Tests verified that the fan motor did not produce ions in sufficient numbers to affect the measurements. Except as noted, all trials for which data are reported here were run with the moist air continuously recirculated by the muffin fan.

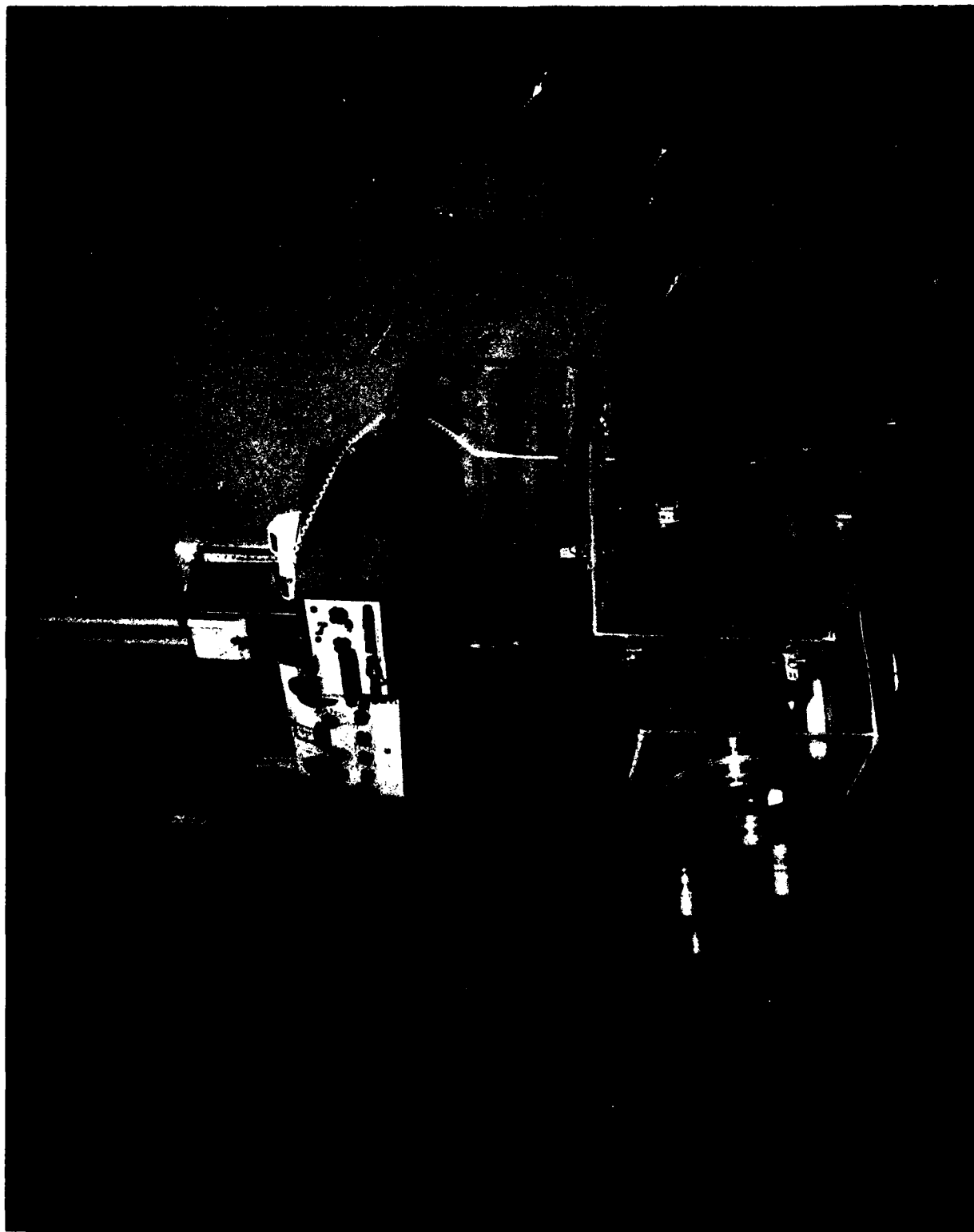Two kinds of experiments were run repeatedly, for which general results are reported. The first kind was designed to determine the maximum values of $I_{cc}$ that could be obtained at s = 1, and thus would represent barrier curve conditions in figure 1. The second kind was designed to see what functional dependencies of $I_{cc}$ vs s would be observed at near-ambient temperatures when liquid water was simply allowed to evaporate in the closed cabinet, and to study the time histories of these dependencies especially when the liquid water container was suddenly removed from the cabinet and the ion population was allowed to decay, thus reflecting the decay of the neutral cluster populations with which the ions were associated. In fact, dissociation into ions could be a primary mechanism by which the neutral clusters gradually decay to their constituent monomers when liquid water is removed from the closed system. This destroys the equilibrium between cluster evaporation and kinetic recondensation of clusters and monomers at the liquid/vapor interface (liquid surface), which accounts for the cluster fraction $(n_c)_v$ shown in figure 1.[9] Without liquid water at equilibrium in the system, the conditions of figure 1 simply are not achieved or maintained. The decay of neutral clusters in the absence of evaporative replenishment is probably similar to the process in the following description: the clusters dissociate into smaller clusters which quickly lose their charges, if any, leaving behind two smaller neutral clusters in place of one original larger one. This brings the mean size of the cluster distribution, $c_u$, more into line with the existing saturation ratio and temperature. The process is repeated until many small neutral clusters remain which have a small overall $c_u$, but make a heavy contribution to $N_{cc}$. Eventually some or all of the clusters revert to monomers, and the product $(N_{cc})$ $(c_u)$ vanishes (equations 11 to 13).

For the first type of experiment, the procedure and results were as follows. With the muffin fan continuously recirculating moist air within the closed cabinet, water was boiled in two large glass beakers in the cabinet, each of which contained an immersion heater. Boiling was allowed to continue for an hour or more, during which the condition s = 1 was assured because the only heat added to the system was that from the boiling water. Enormous values of $I_{cc}$ were recorded by both cells, as is shown by typical data in figure 7 where populations approaching $10^{10}$/cc were measured for temperatures above 50°C, at which point the measurements were discontinued because both cells had such low electrical resistance that essentially the entire source voltage $E_b$ appeared across the voltmeter (E). It is for this reason that the two-plate, single-insulator cells described earlier are needed to continue the measurements to 100°C. Agreement between these measured values of $I_{cc}$ and the theory presented in this paper was excellent, as demonstrated by the following example.

Consider saturated water vapor at 40°C. From figure 1, for the 40°C curve extrapolated to s = 1, $(n_c)_v$ = 0.07. From figure 3, $c_u$ can be estimated as 25 at s = 1 and 40°C. From figure 7, the measured $I_{cc}$ = 7 X $10^8$ at 40°C and s = 1. Therefore, from equation 17, using $K_w$ which was calculated from equation 18, $N_{cc}$ = (1.9 X $10^{15}$)/k, where k is the coefficient in equation 17. Since $N_1$ = 1.7 X $10^{18}$, as shown in equation 11, it is calculated that k = 0.40. This result suggests that if the assumption of ion pair production leading from equation 16 to equation 17 is incorrect, then a value of k = 0.5 would give precise agreement of all parameters, i.e., 2 X k = 1.0 in equation 17,
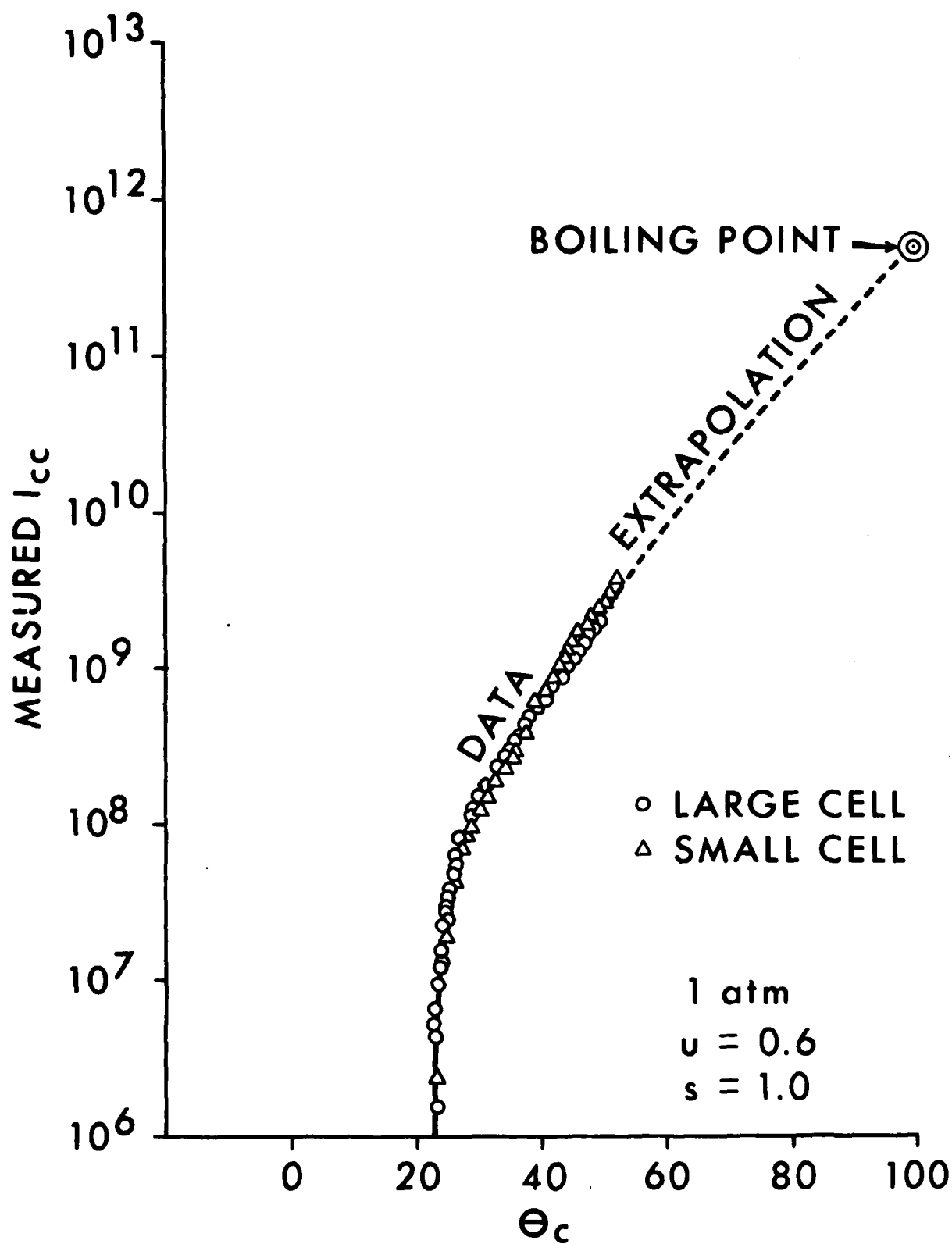
Figure 7. Measured Ion (Charge Carrier) Population Per Cubic Centimeter, $I_{cc}$, at
Saturation (s = 1) for Celsius Temperatures at 1 atm Total Pressure and
Assumed Average Ion Mobility of 0.6 cm$^2$/V-sec

26

and $I_{cc} = \sqrt{K_w}$ ($N_{cc}$) directly. Such agreement seems hardly likely to be fortuitous. Furthermore, it is possible that the assumption of ion pair production is inconsistent in the methodology employed in this paper, simply because the $\beta$ radiation source does indeed break off a tiny fragment or "loose end," such as an OH⁻ molecule, which has such a high mobility compared to the $H^+(H_2O)_c$, even when hydrated, that it does not contribute significantly to the measurement of $I_{cc}$. It would be interesting to see whether detailed calculations for the "ion pair" $(H_2O)_{c+1} \xrightarrow{\beta} H^+(H_2O)_c + OH^-$. for example, would show that the product 2 X k in equation 17 actually is unity. If so, this would also explain why the ion cluster spectra of figure 2 concur so completely with the known properties of the neutral cluster distributions. These observations seem to indicate that cloud physical calculations of heretofore unimaginable precision might be possible using the new, quantitative theory presented here.

In figure 7, an extrapolation of the data curve, which is known quite precisely, as the clustering of points indicates, shows that at 100°C and s = 1 a value of $I_{cc} = 5 \times 10^{11}$ should be approximately correct. When the single-insulator, two-plate cells described earlier are completed and data for s = 1 at 50° to 100°C can be measured, the author will communicate the results for comparison with the extrapolated curve displayed in figure 7. Recall that the curve is based on an assumed ion mobility of 0.6 cm²/V-sec, and that the curve applies only at 1 atm total pressure.

The second kind of experiment will now be described. This was designed to study growth and decay of $I_{cc}$ vs s under nearly ambient conditions.

Because the laboratory air was exceptionally dry (s = 0.25 to 0.30) during the winter months of early 1981 when these trials were run, it was convenient to begin each series of measurements by venting the cabinet to room air and measuring the starting $I_{cc}$, s and $\theta$ values. Untreated laboratory air was used intentionally for these experiments so that the results might be used directly in our applications. The Teflon-insulated cells have threshhold sensitivities in the range of a few hundred ions/cc ($I_{cc}$) when operated at low bias voltages like $E_b$ = 400 vdc. It follows that ion deposition and other ionic reactions which occur in the normal atmosphere can account for $10^2$ to $10^3$ ions/cc, and are immaterial to the experiments described here, the results of which are attainable only in the presence of liquid water in equilibrium with the vapor. This equilibrium can include not only the existence of saturation vapor pressure at s = 1, but the equilibrium that exists at any s at any instant between the liquid and the vapor in contact with it, that it is humidifying at some evaporative rate. The rates, however, are immaterial in closed systems. But the decay times of $I_{cc}$ (and $N_{cc}$) after liquid water is removed from a closed system are very pertinent, because they show how the length of time of last contact with liquid water affects the cluster content of water vapor or moist air.

Conventional ion counters such as Gerdien tubes do not work well near s = 1 due to insulator leakage and very poor cell factors. The author's Teflon-insulator cells overcame these problems by obtaining good cell factors which compensated for insulator leakage, thus allowing measurements which previously could not be made.

In the humidification experiments, one or more 400-cc glass beakers containing liquid water were placed on the floor of the cabinet shown in figure 6, which contained the Teflon-insulated cells resting on Teflon knife edges. Each beaker contained 200 cc of water and a wick consisting of three 24- X 27-cm brown paper towels rolled and placed on end to carry water above the beaker and into the airstream (which averaged 0.6 m/sec velocity when the recirculating muffin fan was in use)

to enhance evaporation. Slow humidification and near-equilibrium conditions were achieved with one beaker in the cabinet, and fast humidification at some cost to equilibrium with three beakers. Saturation ratio was measured by a pair of matched wet-bulb thermometers, and a precision electronic thermometer probe (dry bulb), placed near the beaker(s).

Because cluster and ion phenomena being investigated here are temperature phenomena and not saturation phenomena, the measurement of saturation ratio in these experiments was not critical, for reasons that were discussed earlier, and unsophisticated techniques could be used, for example, simple wet and dry bulb thermometers. The values of $I_{cc}$ vs s, as will be shown, always have similar functions. If the humidity is known within a few percent, it does not affect the results appreciably. After periods which could last several hours at room temperatures, even small amounts of liquid water in the cabinet, which was closed off to room air and usually had the recirculating fan running, could support respectable neutral cluster and ion (charge carrier) populations by their evaporation. The evaporation rate is, of course, slow for small sources of liquid water, and recirculation of the moist air using the fan increases the evaporation rate, as would be expected. Sophisticated experimental technique, such as mounting a thermostat in the cabinet, was simply unwarranted. In fact, all of the ion measurement experiments described here are simple and reproducible, and they can be carried out with uncomplicated equipment because the theory underlying the phenomena which these tests are designed to investigate apparently can now be understood.

Some typical experimental data on humidification are shown in figure 8. These data are for two trials on different days. The 26°C and 29°C temperatures were essentially constant. The solid curve with arrowheads and circular points shows the function of $I_{cc}$ vs s, as humidification took place during a 130-minute period with three beakers, wicks in the cabinet, temperature held at 29°C, and the fan running. For comparison, the dashed curves show the effect of drying of humid air and then rehumidifying it. In this test, only one wick and beaker were used, but a puddle of water 20 cm in diameter was also present on the cabinet floor to simulate standing water. Starting at the solid point where $I_{cc} = 2 \times 10^5$ ions/cm$^3$ and s = 0.77, the air was dried to s = 0.36 over a period of 8 minutes by venting the cabinet to room air; the ion count fell to $2.5 \times 10^4$/cm$^3$. The vent was then closed, and the recirculating 26°C air was rehumidified by evaporation sources. The curve on figure 8 now begins to pass through the solid point from which it started and continues upward along a diagonal, which as the reader probably suspects by now, is very similar to the fine nearly vertical dashed curve between the proposed barrier and condensation curves of figure 1; as previously discussed, this is the proposed barrier curve corrected to $I_{cc}$ due to the extreme tempreature dependency of the dissociative ion product of water (equation 18).

At values of s to the left of the barrier in figure 8, $I_{cc}$ in these experiments had dependencies on s ranging from (s)$^1$ to (s)$^2$. This is consistent with the new theory presented earlier in this paper. Then, at some point approaching the barrier conditions (at an s dependent on the temperature $\theta$), the functions would reach a "knee," as can be seen in figure 8. Note that once they merge the curves climb together with the slope of the dashed $I_{cc}$ curve in figure 1, which can be approximated by (s)$^{11}$. It is clear that if humidification were carried completely to "hard" saturation at s = 1, values of $I_{cc}$ shown in figure 7 for temperatures of 26°C and 29°C would be expected. Thus, even the large ion counts attained by evaporation and exceeding $10^6$/cc, as shown in figure 8, were still 20 to 50 times smaller than their maximum possible values at full saturation.
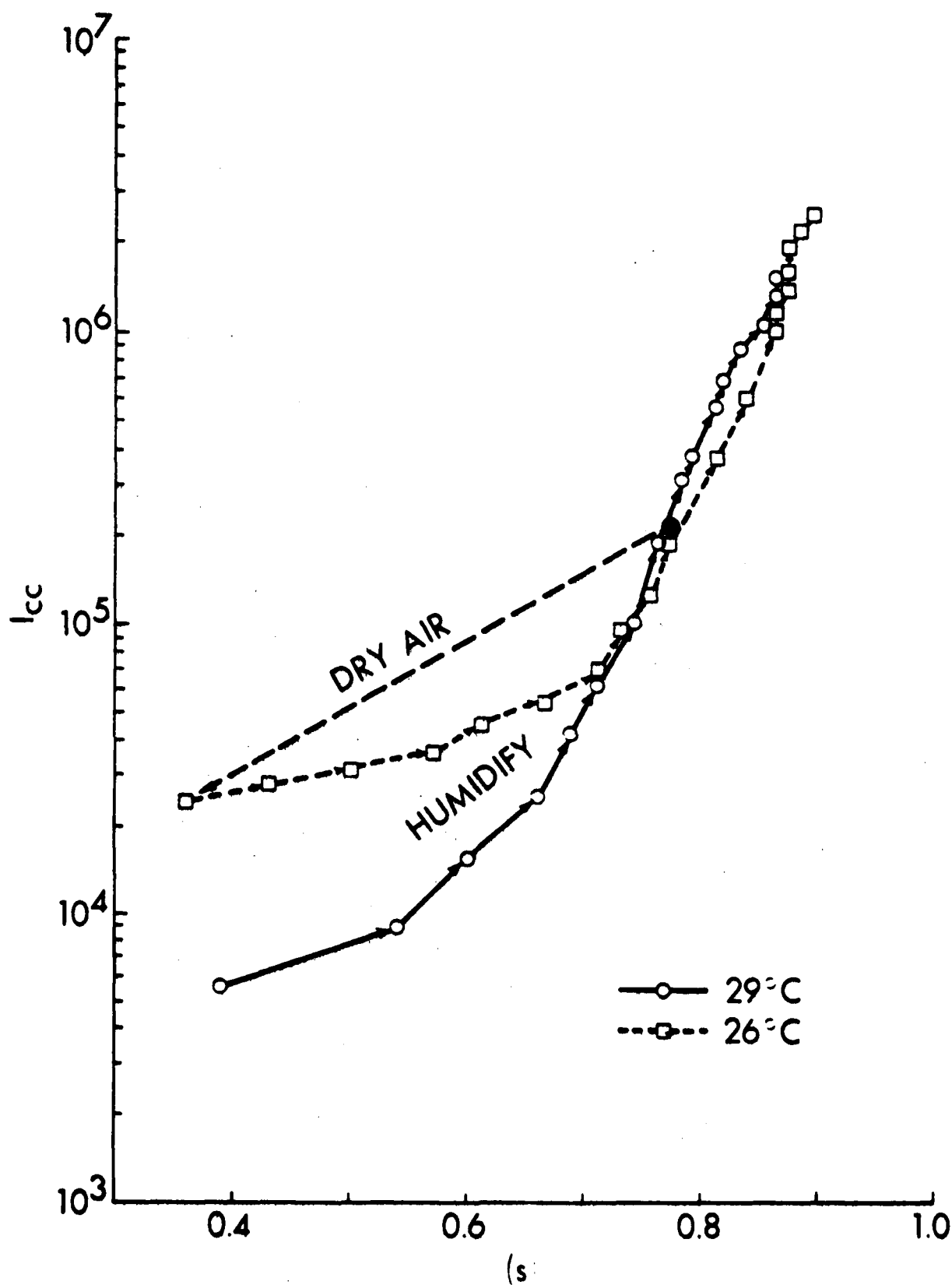
28

Figure 8. $I_{cc}$, Ion Population Per Cubic Centimeter, vs Saturation
Ratio for Experimental Trials on Two Different Days

Figure 9 shows the time history of the data presented in figure 8, plus additional data taken at 29°C after the beakers and wicks were abruptly removed from the test cabinet, which ensured that no liquid water was in contact with moist air to replenish the neutral cluster population by evaporation; hence, the equilibrium dissociative ion population ($I_{cc}$) began to decay. The dashed curve for 26°C descends rapidly in the first 8 minutes as the air was vented to dry room air (also shown by the "dry air" curve in figure 8). The curves then ascend together with a time constant for $1 - 1/e$ (or 63.2% of final value) of approximately $\tau = \sim 150$ minutes, reflecting the evaporation rates that existed in these particular experiments. At an elapsed time of 130 minutes, corresponding to the removal of all wicks and liquid water from the test cabinet, the 29°C (solid) curve in figure 9 begins to decend as the ion population decays. This is not a drying process, however, and should not be confused with the exercise of venting the cabinet to room air, described previously. While some moisture is lost over a period of hours (see "s" notations below the right-hand curve portion in figure 9), some of this probably can be accounted for by the ionization processes themselves. For example, keeping the bias ($E_b = 400$ vdc) applied to the cells continuously, as was done in these experiments, helps to deplete ions which would otherwise contribute to $I_{cc}$. Other experiments showed this depletion to be about 20% of the $I_{cc}$ value that would be measured otherwise. This would represent a very small correction to figure 9. However, this depletion also means that the depleted ions must be made up from the remaining water vapor since the liquid evaporative source of new clusters is no longer present. This could result in a more significant correction to the curve in figure 9. As a precaution, the author has recently adopted the precaution in these measurements of attaching electrical connection to the cells (i.e., to the voltmeter in series with the power supply (bias source) as in figure 5) only at the moment of measurement. The decay time constant shown in figure 9 is approximately $\tau = 40$ minutes, and this order of magnitude is consistent with the decay time of spurious (cluster) infrared emissions from cooling steam.[16]

## 4.    DISCUSSION AND CONCLUSIONS

Taken individually, the elements of the proposed new cloud physics (or microphysics) theory presented in this paper can, in some cases, be explained or rationalized by traditional or classical models of the phenomena that they describe. But taken collectively, the proposed theory seems self-consistent and quite precise so that it should be given serious consideration. The traditional models of cloud physics have been accepted for so long that they have not been seriously questioned for years. After years of acceptance, it is difficult to believe that they could be misleading.

But there is a powerful counter-argument to this unassailability. Why was dT/dr taken as zero in the Thomson equation? Why was it assumed that only monomers evaporate from liquid water according to kinetic theory even though C. T. R. Wilson saw evidence of large clusters even in his earliest work? When hydrogen bonding was discovered, why was there no reexamination of its impact on classical cloud microphysics? Why are the absurdly small populations of neutral clusters that are assumed by homogeneous nucleation theory to have been grown by molecular collisions thought to explain water droplet nucleation? Wilson knew before the turn of the century the more likely and intuitively satisfying state of things: the large neutral cluster "nuclei" in huge numbers are already there in the vapor. How can "supersaturation" exist if saturation vapor pressure is a physical constant of nature at any temperature? Why, in 1983 are we still trying to fit experimental data obtained from marvelous instrumentation into a 100-year-old theoretical framework that was based on largely wrong assumptions and missing information to begin with? Certainly, that missing information must include the extensive hydrogen bonding of water.

30

Figure 9. $I_{cc}$, Ion Population Per Cubic Centimeter vs Elapsed Time in Minutes

For example, the time history of the experimental trials shown in figure 8; time constants, $\tau$, for humidification and decay (after removal of liquid water from the closed system) are shown.

Like the reader, and probably more so, the author feels the weight of the implications of the research reported in this paper. It is heretical to be sure, but the author concludes that traditional models of cloud microphysics may be incorrect, that nucleation may be a temperature phenomenon and not a "supersaturation" one so that cloud nucleation can occur in completely clean moist air simply by cooling it to its nucleation temperature, and that the formalism and measurement techniques set forth in this paper can be applied anywhere by anyone with the expectation of supportive results.

The reader will have to choose for himself.

# LITERATURE CITED

1. J. G. Wilson. The Principles of Cloud Chamber Technique. University Press, Cambridge. 1951.

2. C. T. R. Wilson. Philos. Trans. R. Soc. London 189, 265 (1897).

3. C. T. R. Wilson. Philos. Trans. R. Soc. London 192, 403 (1899).

4. F. F. Abraham. Homogeneous Nucleation Theory. Academic Press, New York. NY. 1974.

5. W. A. P. Luck. In Chapter 5, Water: A Comprehensive Treatise. Vol. 1. p 210. F. Franks, ed., Plenum Press, New York, NY. 1972.

6. H. R. Carlon. Limits of Detection for Condensation Nuclei Counters. J. Appl. Phys. 52. April (1981). Erratum reprinted J. Appl. Phys. 53, 6492 (1982).

7. D. Hadzi, ed. Hydrogen Bonding. Pergamon Press, New York, NY. 1959.

8. L. Pauling. The Structure of Water. Chapter 1 in Reference 7.

9. J. H. deBoer. The Dynamical Character of Adsorption. p 16. Oxford Press. Clarendon, England. 1953.

10. H. R. Carlon and C. S. Harden. Appl. Opt. 19, 1776 (1980).

11. H. R. Carlon. Appl. Opt. 20, 1316 (1981).

12. H. R. Carlon. Infrared Absorption by Molecular Clusters in Water Vapor. J. Appl. Phys. 52, May (1981).

13. H. R. Carlon. J. Atmos. Sci. 36, 832 (1979).

14. H. R. Carlon. Infrared Phys. 19, 549 (1979).

15. H. R. Carlon. Appl. Opt. 10, 2297 (1971).

16. H. R. Carlon. Infrared Phys. 19, 49 (1979).

17. H. R. Carlon, Appl. Opt. 17, 3193 (1978).

18. H. R. Carlon. Appl. Opt. 17, 3192 (1978).

19. K. J. Bignell. Q. J. R. Meteorol. Soc. 96, 390 (1970).

20. H. R. Carlon. Appl. Opt. 20, 726 (1981).

21.    J. L. Kassner, Jr., and D. E. Hagen.  J. Chem. Phys. *64*, letters section, 15 Feb (1976).

22.    J. Q. Searcy, and J. B. Fenn.  J. Chem. Phys. *61*, 5282 (1974).

23.    W. Holzapfel.  J. Chem. Phys. *50*, 4424 (1969).

24.    H. R. Carlon.  J. Appl. Phys. *51*, 171 (1980).

25.    H. R. Carlon.  Ionic Equilibria and Decay Times of Neutral Water Clusters in Moist Air.  J. Appl. Phys. *52*, March (1981).

26.    J. A. Chalmers.  Atmospheric Electricity.  pp 86-88.  Pergamon Press, New York, NY.  1967.

27.    A. D. Moore, ed.  Electrostatics and Its Applications.  p 390.  John Wiley & Sons. New York, New York.  1973,

| Names | Copies | Names | Copies |
|---|---|---|---|
| **CHEMICAL SYSTEMS LABORATORY** | | | |
| | | Federal Emergency Management Agency | |
| ATTN: DRDAR-CLB | 1 | Office of Research/NPP | |
| ATTN: DRDAR-CLB-C | 1 | ATTN: David W. Bensen | 1 |
| ATTN: DRDAR-CLB-PO | 1 | Washington, DC 20472 | |
| ATTN: DRDAR-CLB-R | 1 | | |
| ATTN: DRDAR-CLB-R(M) | 1 | HQ DA | |
| ATTN: DRDAR-CLB-R(S) | 1 | Office of the Deputy Chief of Staff for | |
| ATTN: DRDAR-CLB-T | 1 | Research, Development & Acquisition | |
| ATTN: DRDAR-CLC-B | 1 | ATTN: DAMA-CSS-C | 1 |
| ATTN: DRDAR-CLC-C | 1 | Washington, DC 20310 | |
| ATTN: DRDAR-CLC-E | 1 | | |
| ATTN: DRDAR-CLF | 1 | HQ Sixth US Army | |
| ATTN: DRDAR-CLJ-R | 1 | ATTN: AFKC-OP-NBC | 1 |
| ATTN: DRDAR-CLJ-L | 2 | Presidio of San Francisco, CA 94129 | |
| ATTN: DRDAR-CLJ-M | 1 | | |
| ATTN: DRDAR-CLN | 1 | Commander | |
| ATTN: DRDAR-CLT | 1 | DARCOM, STITEUR | |
| ATTN: DRDAR-CLW-C | 1 | ATTN: DRXST-STI | 1 |
| ATTN: DRDAR-CLW-P | 1 | Box 48, APO New York 09710 | |
| ATTN: DRDAR-CLY-A | 1 | | |
| ATTN: DRDAR-CLY-R | 7 | Commander | |
| | | USASTCFEO | |
| **COPIES FOR AUTHOR(S)** | | ATTN: MAJ Mikeworth | 1 |
| Research Division | 1 | APO San Francisco 96328 | |
| RECORD COPY: DRDAR-CLB-A | 1 | | |
| | | Commander | |
| **DEPARTMENT OF DEFENSE** | | US Army Nuclear & Chemical Agency | |
| | | ATTN: MONA-WE | 1 |
| Defense Technical Information Center | | 7500 Backlick Rd, Bldg 2073 | |
| ATTN: DTIC-DDA-2 | 12 | Springfield, VA 22150 | |
| Cameron Station, Building 5 | | | |
| Alexandria, VA 22314 | | Army Research Office | |
| | | ATTN: DRXRO-CB (Dr. R. Ghirardelli) | 1 |
| Director | | P.O. Box 12211 | |
| Defense Intelligence Agency | | Research Triangle Park, NC 27709 | |
| ATTN: DB-4G1 | 1 | | |
| Washington, DC 20301 | | OFFICE OF THE SURGEON GENERAL | |
| | | | |
| Commander | | Commander | |
| USASED, USAINSCOM | | US Army Medical Bioengineering Research | |
| ATTN: IAFM-SED-III | 1 | and Development Laboratory | |
| Fort Meade, MD 20755 | | ATTN: SGRD-UBD-AL, Bldg 568 | 1 |
| | | Fort Detrick, Frederick, MD 21701 | |
| **DEPARTMENT OF THE ARMY** | | | |
| | | Commander | |
| HQDA | | USA Medical Research Institute of | |
| ATTN: DAMO-NCC | 1 | Chemical Defense | |
| ATTN: DAMO-NC/COL Robinson (P) | 1 | ATTN: SGRD-UV-L | 1 |
| WASH DC 20310 | | Aberdeen Proving Ground, MD 21010 | |

US ARMY MATERIEL DEVELOPMENT AND
    READINESS COMMAND

Commander
US Army Materiel Development and
    Readiness Command
ATTN:  DRCLDC                                    1
ATTN:  DRCSF-P                                   1
5001 Eisenhower Ave
Alexandria, VA  22333


Project Manager Smoke/Obscurants
ATTN:  DRCPM-SMK-S                               3
Aberdeen Proving Ground, MD  21005


Commander
US Army Foreign Science & Technology Center
ATTN:  DRXST-MT3                                 1
220 Seventh St., NE
Charlottesville, VA  22901


Director
US Army Materiel Systems Analysis Activity
ATTN:  DRXSY-MP                                  1
ATTN:  DRXSY-CA (Mr. Metz)                       1
Aberdeen Proving Ground, MD  21005


Commander
US Army Missile Command
Redstone Scientific Information Center
ATTN:  DRSMI-RPR (Documents)                     1
Redstone Arsenal, AL  35809


Director
DARCOM Field Safety Activity
ATTN:  DRXOS-C                                   1
Charlestown, IN  47111


Commander
US Army Natick Research and Development
    Laboratories
ATTN:  DRDNA-O                                   1
ATTN:  DRDNA-IC                                  1
ATTN:  DRDNA-IM                                  1
ATTN:  DRDNA-ITF (Dr. Roy W. Roth)              2
Natick, MA  01760


US ARMY ARMAMENT RESEARCH AND
    DEVELOPMENT COMMAND

Commander
US Army Armament Research and
    Development Command
ATTN:  DRDAR-LCA-L                               1
ATTN:  DRDAR-LCE-C                               1
ATTN:  DRDAR-LCU-CE                              1
ATTN:  DRDAR-NC (COL Lymn)                       3
ATTN:  DRDAR-SCA-T                               1
ATTN:  DRDAR-SCM                                 1
ATTN:  DRDAR-SCP                                 1
ATTN:  DRDAR-SCS                                 1
ATTN:  DRDAR-TDC (Dr. D. Gyorog)                1
ATTN:  DRDAR-TSS                                 2
ATTN:  DRCPM-CAWS-AM                             1
Dover, NJ  07801


US Army Armament Research and
    Development Command
Resident Operations Office
ATTN:  DRDAR-TSE-OA (Robert Thresher)           1
National Space Technology Laboratories
NSTL Station, Mississippi  39529


Commander
ARRADCOM
ATTN:  DRDAR-QAC-E                               1
Aberdeen Proving Ground, MD  21010


Commander
USA Technical Detachment                         1
US Naval EOD Technology Center
Indian Head, MD  20640


US ARMY ARMAMENT MATERIEL READINESS
    COMMAND


Commander
US Army Armament Materiel Readiness Command
ATTN:  DRSAR-ASN                                 1
ATTN:  DRSAR-IRW                                 1
Rock Island, IL  61299


Commander
US Army Dugway Proving Ground
ATTN:  Technical Library (Docu Sect)            1
Dugway, UT  84022

| | | |
|---|---|---|
| **US ARMY TRAINING & DOCTRINE COMMAND** | | **US ARMY TEST & EVALUATION COMMAND** | |

US ARMY TRAINING & DOCTRINE COMMAND

Commandant
US Army Infantry School
ATTN: CTDD, CSD, NBC Branch        1
Fort Benning, GA  31905

Commandant
US Army Missile & Munitions Center
    and School
ATTN: ATSK-CM        1
ATTN: ATSK-TME        1
Redstone Arsenal, AL  35809

Commander
US Army Logistics Center
ATTN: ATCL-MG        1
Fort Lee, VA  23801

Commandant
US Army Chemical School
ATTN: ATZN-CM-C        1
ATTN: ATZN-CM-AFL        2
ATTN: ATZN-CM-TPC        2
Fort McClellan, AL  36205

Commander
USAAVNC
ATTN: ATZQ-D-MS        1
Fort Rucker, AL  36362

Commander
US Army Infantry Center
ATTN: ATSH-CD-MS-C        1
Fort Benning, GA  31905

Commander
USA Training and Doctrine Command
ATTN: ATCD-N        1
Fort Monroe, VA  23651

Commander
US Army Armor Center
ATTN: ATZK-CD-MS        1
ATTN: ATZK-PPT-PO-C        1
Fort Knox, KY  40121

Commander
USA Combined Arms Center and
    Fort Leavenworth
ATTN: ATZL-CAM-IM        1
Fort Leavenworth, KS  66027

US ARMY TEST & EVALUATION COMMAND

Commander
US Army Test & Evaluation Command
ATTN: DRSTE-CT-T        1
Aberdeen Proving Ground, MD  21005

DEPARTMENT OF THE NAVY

Chief of Naval Research
ATTN: Code 441        1
800 N. Quincy Street
Arlington, VA  22217

Project Manager
Theatre Nuclear Warfare Project Office
ATTN: TN-09C        1
Navy Department
Washington, DC  20360

Commander
Naval Explosive Ordnance Disposal
    Technology Center
ATTN: AC-3        1
Indian Head, MD 20640

Commander
Naval Surface Weapons Center
Code G51        1
Dahlgren, VA  22448

Chief, Bureau of Medicine & Surgery
Department of the Navy
ATTN: MED 3C33        1
Washington, DC  20372

Commander
Naval Air Development Center
ATTN: Code 2012 (Dr. Robert Helmbold)        1
Warminster, PA  18974

US MARINE CORPS

Commandant
HQ, US Marine Corps
ATTN: Code LMW-50        1
Washington, DC  20380

Commanding General
Marine Corps Development and
    Education Command
ATTN: Fire Power Division, D091        1
Quantico, VA  22134

DEPARTMENT OF THE AIR FORCE

Department of the Air Force
Headquarters Foreign Technology Division
ATTN: TQTR                                          1
Wright-Patterson AFB, OH  45433

ASD/AESD                                            1
Wright-Patterson AFB, OH  45433

AFAMRL/TS
ATTN:  COL Johnson                                  1
Wright-Patterson AFB, OH  45433

AFAMRL/HE
ATTN:  Dr. Clyde Reploggle                          1
Wright-Patterson AFB, OH  45433

HQ AFSC/SDZ                                          1
ATTN:  CPT D. Riediger
Andrews AFB, MD  20334

HQ, AFSC/SDNE                                        1
Andrews AFB, MD  20334

HQ, AFSC/SGB                                         1
Andrews AFB, DC  20334

HQ, NORAD
ATTN:  J-3TU                                         1
Peterson AFB, CO  80914

HQ AFTEC/TEL                                         1
Kirtland AFB, NM  87117

USAF TAWC/THL                                        1
Eglin AFB, FL  32542

AFATL/DLV                                           1
Eglin AFB, FL  32542

USAF SC
ATTN:  AD/YQ                                         1
ATTN:  AD/YQO (MAJ Owens)                            1
Eglin AFB, FL  32542

AD/XRO                                              1
Eglin AFB, FL  32542

USAFSAM/VN
Deputy for Chemical Defense
ATTN:  Dr. F. Wesley Baumgardner                     1
Brooks AFB, TX  78235

AMD/RDTK
ATTN:  LTC T. Kingery
Brooks AFB, TX  78235                                1

AMD/RDSM                                            1
Brooks AFB, TX  78235

AMD/RDSX                                            1
Brooks AFB, TX  78235

OUTSIDE AGENCIES

Battelle, Columbus Laboratories
ATTN:  TACTEC                                        1
505 King Avenue
Columbus, OH  43201

Toxicology Information Center, JH 652
National Research Council                            1
2101 Constitution Ave., NW
Washington, DC  20418

US Public Health Service
Center for Disease Control
ATTN:  Lewis Webb, Jr.                               1
Building 4, Room 232
Atlanta, GA  30333

Director
Central Intelligence Agency
ATTN:  AMR/ORD/DD/S&T                                1
Washington, DC  20505

ADDITIONAL ADDRESSEE

Commandant
Academy of Health Sciences, US Army
ATTN:  HSHA-CDH                                      1
ATTN:  HSHA-IPM                                      2
Fort Sam Houston, TX  78234

38

Commander
217th Chemical Detachment
ATTN:  AFVL-CD                              1
Fort Knox, KY  40121

Headquarters
US Army Medical Research and
    Development Command
ATTN:  SGRD-RMS                            1
Fort Detrick, MD  21701

Stimson Library (Documents)                1
Academy of Health Sciences, US Army
Bldg. 2840
Fort Sam Houston, TX  78234

# END

## FILMED

## 9-83

## DTIC